

Mechanistic Insights into Iridium-Catalyzed Asymmetric Hydrogenation of Dienes

Xiuhua Cui, Yubo Fan, Michael B. Hall,* and Kevin Burgess*^[a]

Abstract: Hydrogenation of 2,3-diphenylbutadiene (**1**) with the chiral carbene–oxazoline–iridium complex **C** has been studied by means of a combined experimental and computational approach. A detailed kinetic profile of the reaction was obtained with respect to consumption of the substrate and formation of the intermediate half-reduction products, 2,3-diphenylbut-1-ene (**2**) and the final product, 2,3-diphenylbutane (**3**). The data generated from these analyses, and from NMR experiments, revealed several facets of the reaction. After a brief induction period (presumably involving reduction of the cyclooctadiene ligand on **C**), the diene concentration declines in a zero-order process primarily to give mono-

ene intermediates. When all the diene is consumed, the reaction accelerates and compound **3** begins to accumulate. Interestingly, the prevalent enantiomer of the monoene intermediate **2** is converted mostly to *meso*-**3** so the enantioselectivity of the reaction appears to reverse. The reaction seems to be first-order with respect to the catalyst when the catalyst concentration is less than 0.0075 M; diffusion of hydrogen across the gas–liquid interface complicates the analysis at higher catalyst concentra-

tions. Similarly, these diffusion effects complicated measurements of reaction rate versus applied pressure of dihydrogen; other factors like stir speed and flask geometry come into play under some, but not all, the conditions examined. Density functional theory (DFT) calculations, using the PBE method, were used to probe the reaction. These studies indicate a *transoid*- η^4 -diene–dihydride complex forms in the first stages of the catalytic cycle. Further reaction requires dissociation of one alkene ligand to give a η^2 -diene–dihydride–dihydrogen intermediate. A catalytic cycle that features Ir³⁺/Ir⁵⁺ seems to be involved thereafter.

Keywords: asymmetric catalysis • carbene ligands • density functional calculations • hydrogenation • iridium

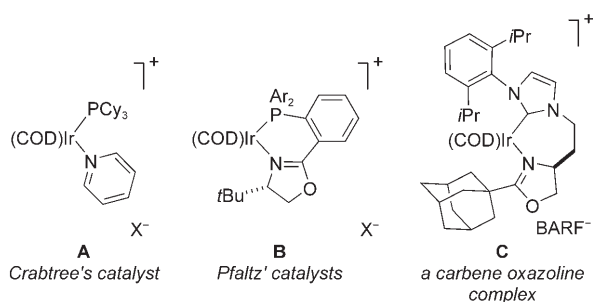
Introduction

From a synthetic perspective, asymmetric hydrogenation of largely unfunctionalized, aryl-substituted monoenes is a maturing field. About a decade ago two catalyst types had emerged that inspired a flurry of interest in this area. One of these was titanium/zirconium catalysts from the Buchwald group, which were shown to give excellent enantioselectivi-

ties and conversions for a broad range of substrate types.^[1–3] However, the subsequent lack of studies indicate others have been reluctant to develop and apply these catalysts, probably because they are not particularly accessible, tend to require 5 mol% loadings, use high hydrogen pressures, and are very air-sensitive. The data obtained by using zirconium-based systems to reduce tetrasubstituted arylalkenes is still the best reported to date,^[3] but subsequent research on hydrogenations of tri- and disubstituted alkenes has focused on iridium-based catalysts. In many cases, these are easier to prepare, moderately air-stable, require only ambient or slightly elevated hydrogen pressures, and are useful at lower catalyst loadings. Thus, using Crabtree's catalyst **A** as a conceptual template,^[4] Pfaltz and co-workers pioneered the application of ligands with N,P-coordinating groups^[5–7] in this area, particularly in phosphine oxazoline complexes like **B**.^[6,8–14] Others,^[14–16] including our group,^[17] subsequently designed and tested similar complexes. More recently, studies from our laboratories demonstrated that *N*-heterocyclic carbene–oxazoline ligands like **C** also could be used to reduce

[a] X. Cui, Y. Fan, M. B. Hall, Prof. K. Burgess
Department of Chemistry, Texas A & M University
P.O. Box 30012, College Station, Texas 77842 (USA)
Fax: (+1) 979-845-8839
E-mail: burgess@tamu.edu

Supporting information for this article is available on the WWW under <http://www.chemeurj.org/> or from the author. The Supporting Information contains the synthetic procedures for **2**, **4**, and **5** providing authentic samples for assignments of absolute configurations; details of the kinetic, NMR, and catalyst screening experiments; and coordinates from the DFT calculations for **P–W**.

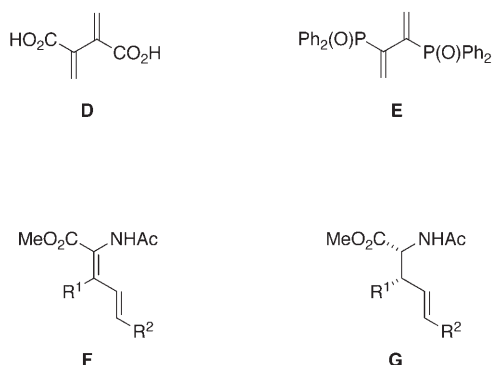


tri- and disubstituted arylalkenes with good conversions and enantioselectivities.^[18,19] The outcome of all these studies is that some iridium-based catalysts are known to mediate reduction of a variety of common, unfunctionalized, trisubstituted arylalkenes, with high conversions and enantioface selectivities. Further modifications to the ligand designs are only likely to give incremental improvements for iridium-catalyzed hydrogenations of these particular substrates.

Despite the interest in iridium-catalyzed hydrogenations of arylalkenes, there are some important unmet goals in the area. Two of these specifically relate to the research described here: 1) reductions of largely unfunctionalized alkenes and 2) elucidation of mechanistic features of the reaction. All the work on iridium-mediated hydrogenations with "Crabtree-like" catalysts has focused on aryl-substituted monoenes, and the mechanism(s) of these reactions remain largely unexplored.

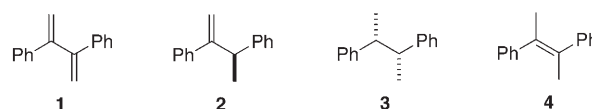
We have identified a logical progression in the field to be asymmetric hydrogenations of dienes (and polyenes). These tend to be more difficult substrates to explore than monoenes, because both relative and absolute stereochemistries must be controlled if two or more chiral centers are formed. However, the rewards are greater if this can be achieved. This is because the chirons that could be generated are more complex, less accessible through other routes, but still potentially useful in stereoselective syntheses.

Surprisingly, the literature reveals little prior art with respect to asymmetric hydrogenations of dienes of any kind. Reduction of the diacid **D** had been explored, with moderate success,^[20] while conversions and enantioselectivities for the di(phosphine oxide) **E** were found to be considerably better.^[21] Both these studies featured functionalized dienes



and ruthenium–BINAP catalysts. Besides these examples, Burk and co-workers had explored rhodium-mediated hydrogenation of the substrates **F** (and isomers);^[22] only the α,β -double bond was reduced giving the products **G**, so in a sense these are archetypical reductions of dehydroamino acids, that is, of well-studied, appropriately functionalized, monoenes. We have not been able to find any other examples of asymmetric reductions of dienes prior to our work.

As an initial study, we chose 2,3-diphenylbutadiene (**1**) as a substrate. It was predictable that stereocontrol for reduction of this particular diene would be difficult because each



alkene unit in it is 1,1-disubstituted, and reduction of this type of alkene tends to be difficult to achieve with high face selectivities. In any case, the products, isomers of 2,3-diphenylbutane, have no evident immediate synthetic applications. Nevertheless, we regarded this as a useful starting point for our investigations, because so many unknowns surrounded the hydrogenation of even this simple diene. Those unknowns can be highlighted by the following questions. Could the reaction be manipulated to give the optically active product **3** with high enantiomeric excess? If so, what is the diastereoselectivity of the process? What are the relative rates of hydrogenation of the two double bonds, and do the monoenes **2** accumulate in the reaction? Related to this, what are the kinetic factors that control the overall stereoselectivity of the reaction? Is the reaction complicated by double bond migration to give the tetrasubstituted alkene **4**? Can any inferences be drawn from these studies regarding the mechanism of iridium-mediated hydrogenations of aryl-substituted monoenes? In the event, all these issues can be addressed, at least to some extent. Our investigations of 2,3-diphenylbutadiene (**1**), which we initially anticipated would be relatively superficial,^[23] evolved into an in-depth and revealing study.

Results and Discussion

The strategy in this project was as follows. Stereochemical assignments were made for the products and intermediates of the reduction process, then the reaction was followed by means of gas chromatography (GC) to develop a kinetic profile of the relative rates of conversion. These observations were supported by a competition experiment to reveal the origin of a small amount of *meso*-**3** that formed in the early stage of the reaction, and by NMR analyses of catalyst/hydrogen, catalyst/substrate mixtures. A series of experiments was then performed using different stirring speeds to explore if hydrogen diffusion effects can alter the outcome of the reaction, then dependencies on catalyst concentration

and hydrogen pressure were investigated. All these experiments were performed with a carbene–oxazoline catalyst that had previously proved to be a preferred one for asymmetric hydrogenations of aryl-substituted monoenes. The last phase of the study was to screen a small library of alternative carbene–oxazoline catalysts to probe for increased stereoselectivities.

In parallel with the experiments described above, an extensive series of density functional theory (DFT) calculations were performed to simulate a preferred reaction mechanism. Basically, relative energies of a series of diastereomeric intermediates were calculated to formulate a model of the preferred reaction path and exclude relatively high-energy routes to the products.

Kinetic profile of the reaction under typical conditions: Two approaches were used to establish the absolute stereochemistries of compounds **2** and **3**. First, an authentic sample of **2** was prepared by a Wittig reaction on the corresponding ketone, which was in turn made using an asymmetric synthesis.^[24] Second, two literature reports describe close and significant optical rotations for compound **3**,^[25,26] hence it was possible to determine the stereochemistry of the material formed in the test reaction by means of polarimetry and correlation. These two approaches were complementary and led to the same conclusions.

Figure 1 gives the reaction conditions used to develop a kinetic profile of the hydrogenation process, the relative rates determined from GC analyses, and the absolute stereochemistries of the compounds involved. This experiment was repeated several times and gave consistent results.

After an induction period of about 4 min, the reaction proceeds at a steady rate indicative of zero-order consumption of diene. In the first 475 min of the hydrogenation, until all the diene **1** is consumed, the monoenes **2** and *ent*-**2** are the major products with the former prevailing, but only in an enantiomeric excess of approximately 12%. It is the events after the diene is consumed that largely govern the enantiomeric excess of the product **3** formed at the end of the reaction. Two matched/mismatched pairs should be considered at the critical point when all the diene is consumed. The catalyst interacts constructively with substrate **2** to give *meso*-**3**, and *ent*-**3** is only formed slowly in that reaction. Conversely, the favored product from *ent*-**2** is the optically active product **3**, and *meso*-**3** only forms from this substrate at about half the rate. The reaction generates an enantiomeric excess of **3**, because the major alkene **2** formed when the diene is consumed is rapidly drained off to *meso*-**3**; simultaneously, the minor enantiomer of the alkene intermediate, *ent*-**2**, preferentially gives **3** that emerges as the preferred enantiomer from the reaction.

Several features of the data shown in Figure 1 are interesting. These are 1) a significant concentration of *meso*-**3**, but not *ent*-**3**, is formed in the first phase of the reaction; 2) small quantities of the double-bond migration product **4** are formed in the first phase of the reaction, but its *Z* isomer is not formed, and the concentration of **4** remains constant in

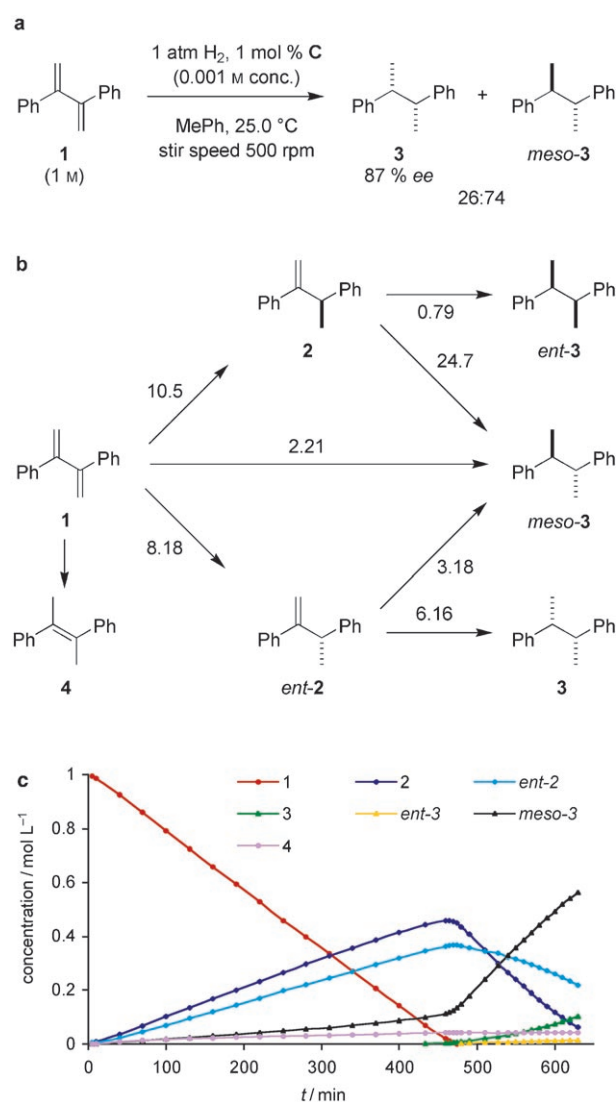


Figure 1. a) The test reaction; b) hydrogenation of 2,3-diphenylbutadiene **1**, with rates in units of $10^{-4} \text{ mol L}^{-1} \text{ min}^{-1}$; and c) concentrations of the reaction components as the reaction proceeds.

the second phase of the reaction; and 3) the enantiomeric excess of **2** formed in the first phase of the reaction is not constant. These observations are now discussed in more depth.

Competition experiment to probe dissociation of the substrate from the metal:

Formation of *meso*-**3** in the first phase of the reaction could occur through two consecutive addition reactions of H_2 to the diene without dissociation of the substrate from the metal. Alternatively, partial hydrogenation of **1** could occur, followed by dissociation to free **2** and *ent*-**2** then recombination of these with the metal to give *meso*-**3**. These two possibilities are expressed in Figure 2a. A competition experiment was devised to distinguish between these two pathways. This was not straightforward, because, by definition, the diene has to be present in the first phase of the reaction. Consequently, conditions were designed, as

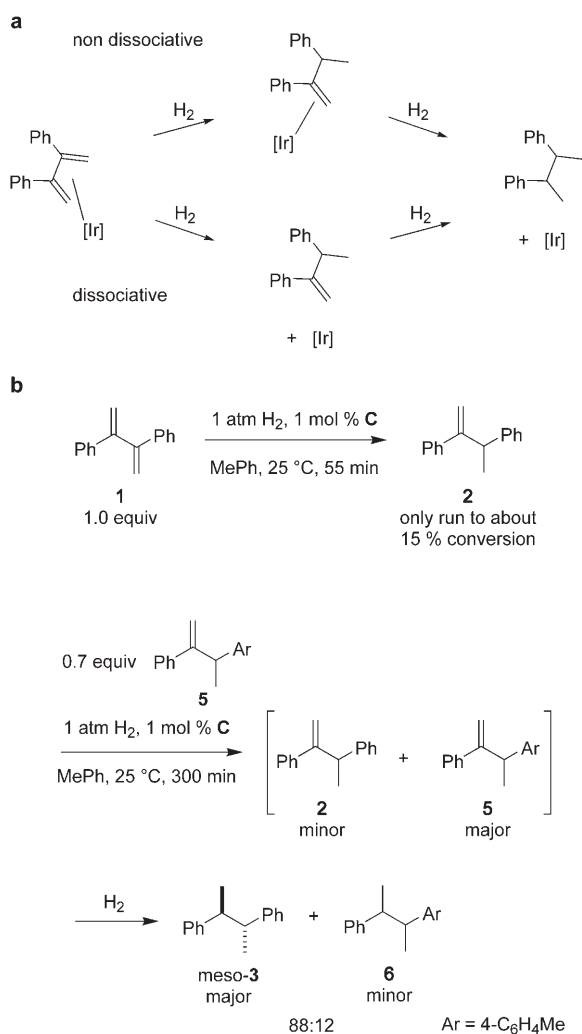


Figure 2. a) Simple representation of dissociative and nondissociative routes to *meso*-3 in the first phase of the reaction and b) a competition experiment showing that the nondissociative mechanism is favored, but both are operative.

shown in Figure 2b, whereby **2** was generated, then an excess of the tolyl derivative **5** was added. Hydrogenation of this mixture gave a disproportionately large amount of *meso*-3. This was not due to faster reaction of *rac*-**2** than *rac*-**5**, because control experiments showed the opposite; *rac*-**5** under our standard reaction conditions was hydrogenated slightly faster than *rac*-**2**. Thus the overall conclusion is that both the nondissociative and the dissociative pathways are operative for the formation of *meso*-3 in the first phase of the reaction, but the nondissociative mechanism is dominant.

The other two unusual features of the kinetic data, that is, in the first phase of the reaction the small quantities of the double-bond migration product **4** formed and the variation of the enantiomeric excess of **2** seem to be related. Evidence for this assertion is as follows. The concentration of the tetrasubstituted alkene **4** varied as shown in Figure 3a. The enantiomeric excess of the monoene **2** varied as shown in Fig-

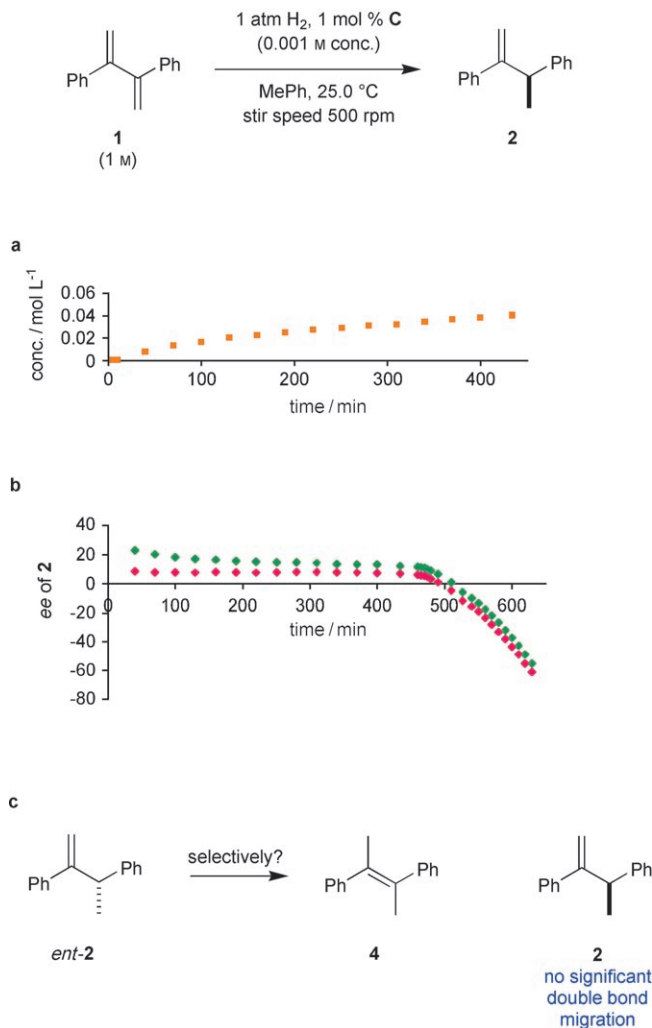


Figure 3. a) Concentration of alkene **4** under the conditions shown in Figure 1a; b) enantiomeric excess of **2** throughout the reaction, shown in green, $ee\% = (2-ent-2)/(2+ent-2) \times 100$; and the enantiomeric excess of **2** adjusted for production of **4** from only *ent*-**2**, shown in pink, $ee\% = (2-(ent-2+4))/(2+(ent-2+4)) \times 100$ as indicated in part c).

ure 3b (green line) during the same time period. We were curious about this unusual variation in enantiomeric excess of **2** and realized that if it were assumed that the tetrasubstituted alkene **4** arose solely from *ent*-**2** then the *ee* of **2** corrected for this is almost constant in the first phase of the reaction (Figure 3b, pink line). We conclude that under these particular conditions **4** may be formed preferentially from *ent*-**2**.

NMR experiments: NMR data were collected in two solvent systems: CDCl₃ and CD₃C₆H₅. Deuteriochloroform was chosen because it is a common solvent for these hydrogenation reactions, (though it was not the one used in the kinetic experiments), and because no solubility issues arose. Deuterated toluene was used to correspond with the medium used for the kinetic experiments, but in this case material tended to separate from the solution as an oil (vide infra). In both solvents, treatment of catalyst **C** with 25 equivalents of

diene **1** for 12 h at 25 °C gave no significant change in the ^1H NMR spectrum indicating that hydrogen is required to displace the cyclooctadiene (COD) ligand.

When catalyst **C** in CDCl_3 was treated with hydrogen under atmospheric pressure in the absence of diene, the ^1H NMR spectrum of the solution changed significantly over a period of approximately 40 min. During this time the resonances attributed to the COD ligand disappeared and a peak corresponding to cyclooctane appeared, but the resonances due to the catalyst were indicative of formation of a mixture of products. No significant hydrogenation occurred when diene was added to this solution. We infer from these experiments that the catalyst is rapidly deactivated in essentially non-coordinating solvents in the absence of alkene substrate. It seems likely that degradation to oligometallic clusters occurred under these conditions, similar to Crabtree's catalysts^[4,27,28] and their chiral phosphine–oxazoline analogues.^[29] However, at the present time we have no evidence to support this for the particular case of catalyst **C**; our efforts to isolate and crystallize these species using similar conditions have been unsuccessful.

When the hydrogenation reaction of diene **1** was performed with diene present from $t=0$ in CDCl_3 , the proton NMR spectra were different to those described above. They were complicated to interpret, except the hydride region showed only one resonance ($\delta = -15.4$ ppm); this signal was not observed in the reaction of catalysts with hydrogen alone. Thus the overall conclusion from these experiments is that both diene (or alkene) and hydrogen are required to form the active catalyst in these reactions.

In $[\text{D}_8]$ toluene, the catalyst behaved differently. After treatment with 1 atm of hydrogen in the absence of diene for 1 h, the COD ligand is reduced to free cyclooctane, and an oily material separated from the solution. The ^1H NMR spectrum of the complex remaining in solution gave two coupled hydridic resonances at $\delta = -16.00$ and -15.97 ppm ($J = 5.7$ Hz). After prolonged treatment with hydrogen (e.g., 5 h), even more material separated out of the solution, and the resonances of the dissolved material diminished. We infer from this experiment, that an iridium dihydride complex with two inequivalent Ir–H moieties was formed. This is consistent with observations from Pfaltz et al. on their iridium phosphine–oxazoline complexes treated with dihydrogen in THF.^[30] Unlike those phosphine–oxazoline complexes, derivatives of catalyst **C** do not have ^{31}P nuclei, so further structural assignments were relatively difficult. When diene **1** was added to a solution of catalyst **C** that had been pretreated with H_2 (1 atm, 5 h), hydrogenation did occur, that is, contrary to what had been observed for the CDCl_3 solution. However, the product distribution was not the same as that observed in the kinetic experiments (compare with Figure 1). In the experiments outlined in Figure 1, only a small amount of completely reduced product, 2,3-diphenylbutane (**3**), was observed until all the starting material was consumed. However, for the experiment here, in which the catalyst was pre-treated with H_2 , significant amounts of diene **1**, product **3**, and the intermediate half-re-

duction products **2** were observed to co-exist in the same solution. These data indicate that the reaction proceeds somewhat differently under these two sets of conditions. It is possible that solvent coordination effects of toluene are sufficient to stabilize intermediates in the process, whereas decomposition events under similar conditions in CDCl_3 were more prevalent.

For $[\text{D}_8]$ toluene as solvent, the hydrogenation of diene **1** (1 atm H_2 , 20 min, diene present from $t=0$) gave proton NMR spectra that were different to those described above. Just as in the kinetic experiments, only significant quantities of the monohydrogenated intermediates **2** were observed. Resonances associated with the ligand and hydridic region were complicated and difficult to interpret.

Hydrogen diffusion effects: Until this point, the emphasis of these studies had been on the relative rates of reaction under a given set of conditions. The next stage was to consider relationships of the reaction rate to catalyst and hydrogen concentration. However, work by Blackmond and others has highlighted situations in which applied hydrogen pressure and concentration of hydrogen in solution are not always related in a simple way for catalytic hydrogenation reactions.^[31,32] Pfaltz et al. have also noted that H_2 diffusion effects might be important for catalysts formed from their phosphine–oxazolines for cases in which the substrate reacts relatively fast.^[9,33] Further, there is evidence that, unlike some rhodium-catalyzed hydrogenation reactions in which oxidative addition of hydrogen tends to be rate-limiting, the corresponding reactions of cationic Ir^+ complexes tend to be fast even at -80°C .^[34,35] This is to be expected due to the greater thermodynamic stability of Ir–H bonds relative to Rh–H bonds. Thus, there is a possibility that diffusion of hydrogen is rate-limiting. The likelihood that hydrogen diffusion across a gas–liquid interface becomes rate-limiting increases for substrates that are intrinsically fast to react, especially at increased catalyst concentrations and relatively low hydrogen pressures.

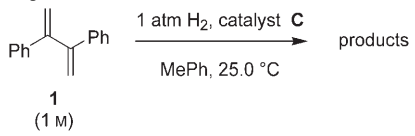
Diene **1** is less reactive than most monoenes that we have tested in the presence of catalyst **C**. For instance, the diene requires reaction times of the order of 10 h, whereas (*E*)-1,2-diphenylpropene under similar conditions, but with less catalyst, required reaction times of only 2 h for complete conversion. This factor implies that hydrogen diffusion rates might not be so important for diene **1** as they are for monoenes.

Experiments to test if the diffusion of hydrogen is rate-limiting or not can feature experiments with different catalyst loadings, vessels with different gas–liquid contact surface areas, and/or experiments with different stir speeds. It was not practical to vary the catalyst loadings in these experiments, because the reaction becomes inconveniently slow when significantly less than 1 mol % of catalyst is used, and competitive deactivation of the catalyst after prolonged reaction times also becomes an issue. Conversely, experiments with high catalyst loadings are not truly representative of the conditions used, and would consume large

amounts of the valuable catalyst **C**. For these reasons, we elected to use stir speeds as a prime method for determining the importance of hydrogen diffusion effects on the reduction of diene **1**. Different vessel geometries were used in some cases to accentuate the effects.

Table 1 shows rates of consumption of diene as a function of various catalyst concentrations and stir speeds in the same reaction vessel. Each value is based on 5–6 data

Table 1. Variance in rate of consumption of diene with catalyst concentration and stir speed.



Entry	Cat. conc. [molL ⁻¹]	stir speed [rpm]	-d[diene]/dt [10 ⁻³ molL ⁻¹ min ⁻¹]
H ₂ diffusion effects unimportant			
1	0.0075	300	1.9
2	0.0075	500	2.0
3	0.0075	700	1.9
4	0.0075	900	2.0
5	0.0075	1100	2.0
borderline region			
6	0.01	500	2.2
7	0.01	700	2.6
8	0.01	1100	2.6
H ₂ diffusion effects important			
9	0.015	300	2.5
10	0.015	700	3.4
11	0.015	1100	4.2

points, and nearly all the experiments were performed twice. The data show that at the catalyst concentration 0.0075 M there is no evidence that stir speed effects the measured rate of consumption of the diene (entries 1–5). However, when the catalyst concentration was increased 0.015 M then H₂ diffusion effects were clearly significant (entries 9–11).

The kinetic studies performed early in this work featured catalyst concentrations of 0.010 M. This was a deliberate choice. We desired to keep the reactions rates high enough that the kinetics could be measured conveniently, without encountering excessive complications from H₂ diffusion effects. The data shown in entries 6–8 of Table 1 indicate that this is a borderline region (the vessel used here was the same as for the kinetic experiments). Consequently, a series of control experiments were undertaken to check that H₂ diffusion effects do not significantly affect the outcome of the reaction under these types of conditions. These are now described below.

The first set of experiments used a vessel with a larger gas–liquid interface than the one used in the kinetic experiments, that is, a geometry that does not favor rate-limiting H₂ diffusion. The catalyst concentration was kept at 0.010 M

Table 2. Control experiments for H₂ diffusion effects.^[a]

Entry	Stir speed [rpm]	Conv (1) [%]	yield (3) [%]	ee (3) [%]	dr (3) [%]
1	500	100	95	93	70/30
2	> 1100 ^[b]	100	95	93	71/69

[a] Data shown are the average of two experiments. [b] Maximum stir speed of magnetic stirrer was used.

(just as in the kinetic experiments), and the stir speeds were varied between two extremes. Table 2, entries 1–2 show that the product distribution and stereoselectivities did not vary with stir speed under these conditions, confirming that H₂ diffusion was not determinant in the stereoselectivities under these conditions. The product distribution and stereoselectivities are very close to those observed in the kinetic analyses (Figure 1).

Slight differences in the data obtained from the experiments outlined in Figure 1 and those in Table 2 may indicate small variations in the relative rates would be observed under conditions under which mass-transfer effects were a distant possibility. However, the influence of mass transfer under the conditions shown in Figure 1 is largely inconsequential to the overall conclusions regarding the origin of the optical purity of the product.

Dependence on catalyst concentration: Rates of consumption of the diene **1** were measured at different catalyst concentrations under the conditions indicated in Figure 4a. The same reaction vessel and stir speed were used throughout, so the influence of diffusion rates was constant. The rate of reaction was linearly related to the catalyst concentration: the reaction rate is first-order with respect to the catalyst under these conditions.

Dependence on hydrogen pressure: The experiments with variation of stirring speeds proved that diffusion rates influence the enantioselective hydrogenation of diene **1**. Further, we have already reported that enantiomeric excesses in hydrogenations of some, but not all, aryl-substituted monoenes can vary with hydrogen pressure.^[19] This observation is indicative of a change in the relative rates in a given pathway, or perhaps even a more fundamental mechanistic shift. Such mechanistic variations include transitions between situations in which the diffusion of hydrogen is and is not a controlling factor. Significantly, one of the aryl-substituted monoenes for which *ee* and H₂ pressure were related was the 1,1-disubstituted substrate **H**, a compound that is structurally similar to diene **1**. These considerations indicate that only limited inferences can be drawn from the effects of pressure on the rate of the hydrogenation reaction. Nevertheless variance of enantioselectivity with pressure was measured for diene **1** (Figure 4b).

The data shown in Figure 4b for the elevated pressures are the composite sets of experiments (5–6 data points each) repeated four times. They show that the rate of consumption of diene under these conditions appears to be linearly relat-

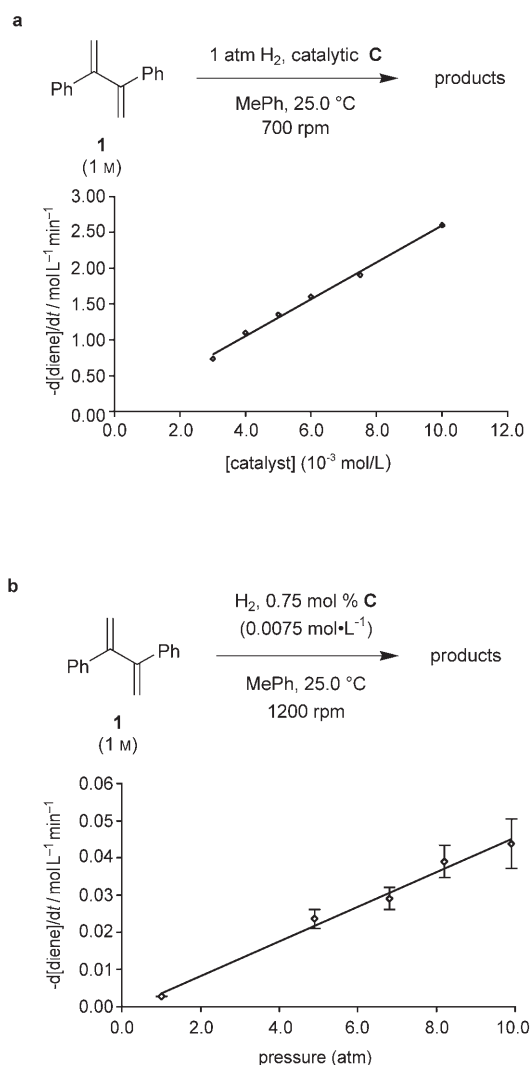
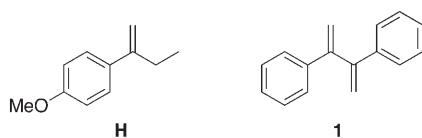


Figure 4. a) Variation of reaction rate with catalyst concentration. Each data point is the average of two sets of experiments (each of 5–6 data points), values obtained from each set of experiments were identical to within 0.1 mol L^{-1} . b) Variation of the rate of the reaction shown with applied hydrogen pressure. Each data point for the elevated pressures is the average of four sets of experiments (each of 5–6 data points); error bars shown indicate one standard deviation.



ed to the applied pressure. However, as indicated above, these observations do not prove first-order rate dependence on hydrogen in the catalytic cycle.

Modeling of the reaction: We recently communicated a detailed DFT computational study of arylalkene hydrogenation mediated by our catalyst **C**.^[36] Both the approach to that modeling study and the conclusions that were reached

are relevant here. Our confidence in that modeling study was reinforced by the good correspondence between calculated and experimental values of enantiomeric excesses.

Our studies on the asymmetric hydrogenation of arylalkenes with catalyst **C** indicated the catalytic cycles favored the key steps shown in Figure 5. After the COD ligand is reduced, the iridium(III)–dihydride–dihydrogen complex **I** is formed. The key steps are rupture of the dihydrogen ligands and formation of a C–H bond and a C–Ir bond via the transition state **J** to give the Ir^{3+} complex **K**, and the reductive elimination process from **K** to **M** via **L**. These steps are calculated to have similar energetics, so either could be turnover-limiting, but only the second one is irreversible. Thus, the cycle features transitions between Ir^{3+} and Ir^{5+} oxidation states but not Ir^{4+} .

Another important aspect of the original modeling study was as follows. The relative energies of the intermediates **I**, **K**, and **M** in the arylalkene hydrogenation corresponded to the relative energies of the transition states **J** and **L** without crossover. This result is also significant, because the intermediates are easier to model than the transition states. Consequently, the relative energies of only the intermediates were modeled in the work described here.

Before the DFT calculations outlined above, two of us had hypothesized that the hydrogenation of 2,3-diphenylbutadiene (**1**) perhaps involved $\text{Ir}^+/\text{Ir}^{3+}$ cycling via an η^4 -diene complex like **N** in the first phase of the reaction, because the diene precludes formation of a dihydride–dihydrogen complex, then, after all the diene is consumed, an $\text{Ir}^{3+}/\text{Ir}^{5+}$ pathway dominates.^[23] The previous set of DFT calculations (for aryl-substituted alkenes) and the ones performed for this study now allow us to revise this hypothesis.

Modeling studies indicate that the diene coordinated in a *transoid* configuration as in **O** (not *cisoid* as in **N**) is preferred (Figure 5b). Optimized geometries of the intermediates reveal the reason for this: the *transoid* form has the phenyl group comfortably resting behind the adamantyl group of the ligand (Figure 5c), whereas the *cisoid* isomer incurs a serious repulsive interaction between an isopropyl group on the ligand and one of the phenyl substituents on the diene (Figure 5d). We also observed that one of the two π -coordinated alkene bonds in the *transoid* form is twisted away from the metal. This seems likely to be the alkene that dissociates to accommodate a hydrogen for reduction to occur through an $\text{Ir}^{3+}/\text{Ir}^{5+}$ pathway. Two possibilities for such an alkene dissociation/ H_2 addition are depicted in Figure 6a. The η^4 -diene complexes (**P** and **R**) are significantly more stable than the corresponding η^2 -forms (**Q** and **S**). This observation accounts for the fact that hydrogenation of the diene in the first phase of the reaction is slower than reduction of the monoenes in the second one. It also explains why the catalyst preferentially coordinates and reduces diene even when monoene is present in the reaction mixture. It is unnecessary to calculate all the intermediates in the reaction, and there are so many possible conformational states beyond this stage that it is not practical to simulate them all in any case. However, none of the trial calculations that

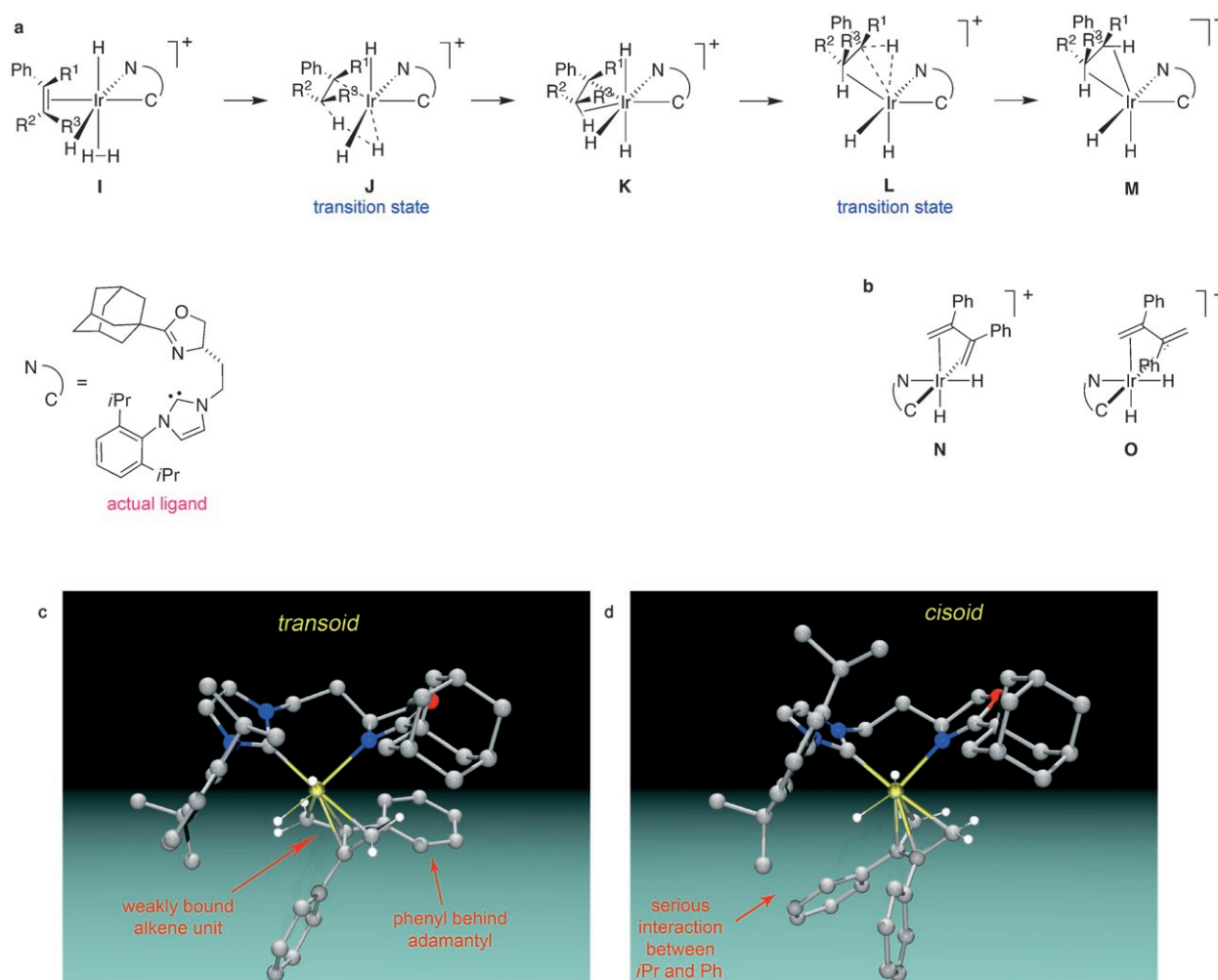


Figure 5. a) The mechanism of hydrogenation of selected arylalkenes by catalyst **C** as modeled using DFT calculations; b) *cisoid* (**N**) and *transoid* (**O**) η^4 -diene complexes; c) calculated structure of the *transoid* intermediate and d) that of the disfavored *cisoid* intermediate.

were performed indicated that $\text{Ir}^+/\text{Ir}^{3+}$ cycling occurs, so that part of our original hypothesis now seems unlikely. Figure 6a illustrates the calculated relative energies for the two diastereomeric *transoid* η^4 -diene complexes, and the corresponding two diastereomeric η^2 -forms after complexation of H_2 . The most stable dihydride dihydrogen complex would lead to the alkene **2** that was actually observed in the reaction (Figure 6b). The relative free energies of the complexed monoene intermediates were also calculated. These relative energies are in accord with the measured reaction rates from the monoene intermediates, that is, formation of *meso-3* is faster than *ent-3* from **2**, and **3** forms faster than *meso-3* from *ent-2*. This supports our assumption that the relative energies of these intermediates correspond to those of the transition states (not calculated) without crossover.

Screening other catalysts: A small library of alternative catalysts was screened for hydrogenation of the diene **1** (Table 3). To accelerate the process, these tests were performed by using 10 atm H_2 pressure. Under these conditions, the enantiomeric excess of the product **3** that was obtained

using catalyst **C** was somewhat depressed (75 vs 87% *ee* at 1 atm). There are indications in the data collected that a superior catalyst for hydrogenation of substrate **1** could be identified. For instance, the catalysts represented in entries 2, 3, and 5 gave higher enantioselectivities and larger **3**:*meso-3* ratios than catalyst **C** under the same conditions. These leads were not pursued further, since the objective of these studies was not to maximize the optical purity of substrate **3**. Nevertheless, the data indicate that catalyst **C** is not necessarily the best possible one for hydrogenations of dienes, even though it was conspicuously good for hydrogenations of aryl-substituted monoenes. This information may be valuable in studies that are ongoing in these laboratories to investigate hydrogenations of dienes and polyenes that give more synthetically useful products.

Conclusion

Assimilation of the experimental and theoretical data accumulated in this study provided a reasonably lucid view of

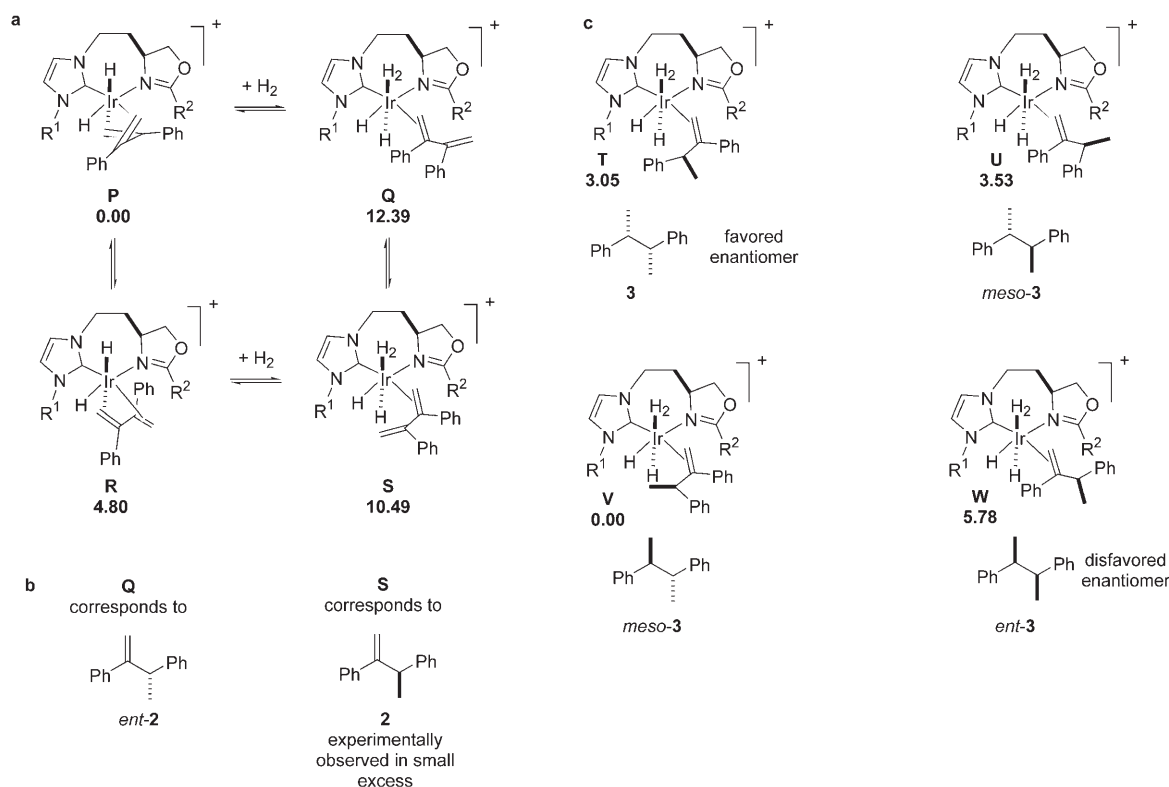


Figure 6. a) Calculated relative free energies (kcal mol⁻¹, **P** as origin) of the four probable intermediates formed in the hydrogenation of diene **1**; b) correlation of the η^2 -forms with the monoenes **2**; and c) relative free energies (**V** as origin) of the complexed monoene intermediates and the reduced products that would arise from these.

Table 3. Screening of alternative catalysts for hydrogenation of diene **1**.

Entry	R ¹	R ^{2[a]}	Conv [%]	products [%]			ee [%] (R,R)- 3	3:meso-3
				2	4	3		
1	2,6- <i>i</i> Pr ₂ C ₆ H ₃	1-Ad	> 99	0	15	85	75	28:72
2	2,6-Et ₂ C ₆ H ₃	1-Ad	> 99	0	5	95	79	36:64
3	2,4,6-Me ₃ C ₆ H ₂	1-Ad	> 99	0	4	96	79	41:59
4	3,5- <i>t</i> Bu ₂ -4-MeOC ₆ H ₂	1-Ad	> 99	0	1	99	86	23:77
5	2,5- <i>t</i> Bu ₂ C ₆ H ₂	1-Ad	> 99	0	5	95	91	31:69
6	2,6- <i>i</i> Pr ₂ C ₆ H ₃	3,5- <i>t</i> Bu ₂ C ₆ H ₃	99	0.4	8	90	-68	8:92
7	2,6- <i>i</i> Pr ₂ C ₆ H ₃	<i>t</i> Bu	13	3	2	8	—[b]	—[b]
8	Ph ₂ CH	<i>t</i> Bu	15	4	0.1	11	—[b]	—[b]
9	Ph ₂ CH	1-Ad	1.0	0.4	0.2	0.7	—[b]	—[b]
10	<i>t</i> Bu	1-Ad	0.5	0.2	0	0.2	—[b]	—[b]

[a] 1-Ad = 1-adamantyl. [b] Not determined due to small quantities involved.

the course of events that lead to products in the hydrogenation of substrate **1**. They also indicate how the mechanism of the reaction can vary, or appear to vary, if some particular experimental parameters are changed. This combined practical and computational approach also point to some key features that are likely to be general to hydrogenations of aryl-alkene substrates by iridium catalysts.

it is quite likely that η^3 -allyl complexes feature in the mechanism of this reaction, and neither the kinetic or DFT experiments can support or refute this idea. Nevertheless, an outline of the mechanistic picture for these reactions is now clear.

The hydrogenation of 2,3-diphenylbutadiene (**1**) with catalyst **C** is initially zero-order in diene and probably first-order in catalyst; however, transfer of hydrogen across the gas-liquid interface becomes an issue at high catalyst concentrations and under conditions that favor relatively slow diffusion of hydrogen into the solution. DFT calculations indicate that an Ir³⁺/Ir⁵⁺ pathway prevails via *trans-oid* η^4 -diene complexes. These must dissociate one alkene group to give an η^2 -complex before the hydrogenation can proceed. These studies do not provide all the details of the reaction mechanism. For instance,

Computational Methods

Briefly, with respect to the computational approach, we showed that there was good agreement with data generated using the B3LYP and PBE methods for arylalkene hydrogenation mediated by catalyst **C**.^[36] That was extremely important because a comprehensive set of B3LYP calculations for the complete structures of the catalyst **C** and of the alkene substrate would have been far too computationally expensive (even using our state-of-the-art facilities), but they are practical using the PBE method.

Methods used in the computational experiments described here build upon the previous approach described above. Thus all the calculations were carried out using the Gaussian 03^[37] implementation of PBE^[38] density functional theories, which for these systems produces results similar to B3LYP.^[39,40] The basis sets used were LANL2DZ with ECP for Ir^[41,42] and D95v for all other elements.^[43] This switch from B3LYP to PBE was made because density-fitting functions^[44,45] can be used with PBE and make these calculations much faster; hence the problem was computationally accessible. Throughout, intermediates were modeled but not the transition states. All structures were fully optimized, and analytical frequency calculations were performed at the same theoretical level on each structure to ensure a minimum was achieved. Zero-point energies and thermodynamic functions were computed for 298.15 K and 1 atm. Only the cation of the complex was modeled.

Acknowledgements

Financial support for this work was provided by The National Science Foundation (CHE-0456449, 98-00184, DMR 02-16275, and 05-18074) and The Robert Welch Foundation (A1121 and A0648). We thank Johnson Matthey plc for help with some precious metals, Dr Shane Tichy and the TAMU/LBMS-Applications Laboratory for MS support, and NMR Laboratory at Texas A&M University, supported by a grant from the National Science Foundation (DBI-9970232) and the Texas A&M University System.

- [1] R. B. Grossman, R. A. Doyle, S. L. Buchwald, *Organometallics* **1991**, *10*, 1501–1505.
- [2] R. D. Broene, S. L. Buchwald, *J. Am. Chem. Soc.* **1993**, *115*, 12569–12570.
- [3] M. V. Troutman, D. H. Appella, S. L. Buchwald, *J. Am. Chem. Soc.* **1999**, *121*, 4916–4917.
- [4] R. Crabtree, *Acc. Chem. Res.* **1979**, *12*, 331–337.
- [5] A. Pfaltz, *Synlett* **1999**, 835–842.
- [6] T. Bunlaksananusorn, K. Polborn, P. Knochel, *Angew. Chem.* **2003**, *115*, 4071–4073; *Angew. Chem. Int. Ed.* **2003**, *42*, 3941–3943.
- [7] G. Helmchen, A. Pfaltz, *Acc. Chem. Res.* **2000**, *33*, 336–345.
- [8] A. Lightfoot, P. Schnider, A. Pfaltz, *Angew. Chem.* **1998**, *110*, 3047–3050; *Angew. Chem. Int. Ed.* **1998**, *37*, 2897–2899.
- [9] D. G. Blackmond, A. Lightfoot, A. Pfaltz, T. Rosner, P. Schnider, N. Zimmermann, *Chirality* **2000**, *12*, 442–449.
- [10] J. Blankenstein, A. Pfaltz, *Angew. Chem.* **2001**, *113*, 4577–4579; *Angew. Chem. Int. Ed.* **2001**, *40*, 4445–4447.
- [11] D. Drago, P. S. Pregosin, A. Pfaltz, *Chem. Commun.* **2002**, 286–287.
- [12] F. Menges, A. Pfaltz, *Adv. Synth. Catal.* **2002**, *344*, 40–44.
- [13] F. Menges, M. Neuburger, A. Pfaltz, *Org. Lett.* **2002**, *4*, 4713–4716.
- [14] P. G. Cozzi, F. Menges, S. Kaiser, *Synlett* **2003**, 833–836.
- [15] G. Xu, S. Gilbertson, *Tetrahedron Lett.* **2003**, *44*, 953–955.
- [16] W. Tang, W. Wang, X. Zhang, *Angew. Chem.* **2003**, *115*, 973–976; *Angew. Chem. Int. Ed.* **2003**, *42*, 943–946.
- [17] D.-R. Hou, J. H. Reibenspies, T. J. Colacot, K. Burgess, *Chem. Eur. J.* **2001**, *7*, 5391–5400.
- [18] M. T. Powell, D.-R. Hou, M. C. Perry, X. Cui, K. Burgess, *J. Am. Chem. Soc.* **2001**, *123*, 8878–8879.
- [19] M. C. Perry, X. Cui, M. T. Powell, D.-R. Hou, J. H. Reibenspies, K. Burgess, *J. Am. Chem. Soc.* **2003**, *125*, 113–123; X. Cui, K. Burgess, *Chem. Rev.*, in press.
- [20] H. Muramatsu, H. Kawano, Y. Ishii, M. Saburi, Y. Uchida, *J. Chem. Soc. Chem. Commun.* **1989**, 769–770.
- [21] V. Beghetto, U. Matteoli, A. Serivanti, *Chem. Commun.* **2000**, 155–156.
- [22] M. J. Burk, K. M. Bedingfield, W. F. Kiesman, J. G. Allen, *Tetrahedron Lett.* **1999**, *40*, 3093–3096.
- [23] X. Cui, K. Burgess, *J. Am. Chem. Soc.* **2003**, *125*, 14212–14213.
- [24] O. Roy, A. Riahi, F. Henin, J. Muzart, *Eur. J. Org. Chem.* **2002**, 3986–3994.
- [25] N. D. Berova, B. J. Kurtev, *Tetrahedron* **1969**, *25*, 2301–2311.
- [26] H. H. Richmond, E. J. Underhill, A. G. Brook, G. F. Wright, *J. Am. Chem. Soc.* **1947**, *69*, 937–939.
- [27] H.-H. Wang, A. L. Casalnuovo, B. J. Johnson, A. M. Muetting, L. H. Pignolet, *Inorg. Chem.* **1988**, *27*, 325–331.
- [28] H.-H. Wang, L. H. Pignolet, *Inorg. Chem.* **1980**, *19*, 1470–1480.
- [29] S. P. Smidt, A. Pfaltz, *Organometallics* **2003**, *22*, 1000–1009.
- [30] C. Mazet, S. P. Smidt, M. Meuwly, A. Pfaltz, *J. Am. Chem. Soc.* **2004**, *126*, 14176–14181.
- [31] Y. Sun, R. N. Landau, J. Wang, C. LeBlond, D. G. Blackmond, *J. Am. Chem. Soc.* **1996**, *118*, 1348–1353.
- [32] Y. Sun, J. Wang, C. LeBlond, R. A. Reamer, J. Laquidara, J. R. Sowa, Jr., D. G. Blackmond, *J. Organomet. Chem.* **1997**, *548*, 65–72.
- [33] S. P. Smidt, N. Zimmermann, M. Studer, A. Pfaltz, *Chem. Eur. J.* **2004**, *10*, 4685–4693.
- [34] B. F. M. Kimmich, E. Somsok, C. R. Landis, *J. Am. Chem. Soc.* **1998**, *120*, 10115–10125.
- [35] R. H. Crabtree, H. Felkin, G. E. Morris, *J. Chem. Soc. Chem. Commun.* **1976**, 716–717.
- [36] Y. Fan, X. Cui, K. Burgess, M. B. Hall, *J. Am. Chem. Soc.* **2004**, *126*, 16688–16689.
- [37] Gaussian 03, Revision B.05, M. J. Frisch, G. W. Trucks, H. B. Schlegel, G. E. Scuseria, M. A. Robb, J. R. Cheeseman, Montgomery J. A. Jr., T. Vreven, K. N. Kudin, J. C. Burant, J. M. Millam, S. S. Iyengar, J. Tomasi, V. Barone, B. Mennucci, M. Cossi, G. Scalmani, N. Rega, G. A. Petersson, H. Nakatsuji, M. Hada, M. Ehara, K. Toyota, R. Fukuda, J. Hasegawa, M. Ishida, T. Nakajima, Y. Honda, O. Kitao, H. Nakai, M. Klene, X. Li, J. E. Knox, H. P. Hratchian, J. B. Cross, V. Bakken, C. Adamo, J. Jaramillo, R. Gomperts, R. E. Stratmann, O. Yazyev, A. J. Austin, R. Cammi, C. Pomelli, J. W. Ochterski, P. Y. Ayala, K. Morokuma, G. A. Voth, P. Salvador, J. J. Dannenberg, V. G. Zakrzewski, S. Dapprich, A. D. Daniels, M. C. Strain, O. Farkas, D. K. Malick, A. D. Rabuck, B. B. Stefanov, G. Liu, A. Liashenko, P. Piskorz, I. Komaromi, R. L. Martin, D. J. Fox, T. Keith, Al-M. A. Laham, C. Y. Peng, A. Nanyakkara, M. Challacombe, P. M. W. Gill, B. Johnson, W. Chen, M. W. Wong, C. Gonzalez, J. A. Pople, Gaussian, Inc.: Willingford, CT, **2004**.
- [38] J. P. Perdew, K. Burke, M. Ernzerhof, *Phys. Rev. Lett.* **1996**, *77*, 3865–3868.
- [39] A. D. Becke, *J. Chem. Phys.* **1993**, *98*, 5648–5652.
- [40] C. Lee, W. Yang, R. G. Parr, *Phys. Rev. B* **1988**, *37*, 785–789.
- [41] P. J. Hay, W. R. Wadt, *J. Chem. Phys.* **1985**, *82*, 270–283.
- [42] W. R. Wadt, P. J. Hay, *J. Chem. Phys.* **1985**, *82*, 299–310.
- [43] T. H. Dunning, P. J. Hay in *Modern Theoretical Chemistry, Vol. 3* (Ed.: H. F. Schaefer III), New York, **1976**.
- [44] B. I. Dunlap, *J. Mol. Struct.* **2000**, *529*, 37–40.
- [45] B. I. Dunlap, *J. Chem. Phys.* **1983**, *78*, 3140–3142.

Received: July 2, 2005
Published online: September 15, 2005